

JAAS

Accepted Manuscript



This is an *Accepted Manuscript*, which has been through the Royal Society of Chemistry peer review process and has been accepted for publication.

Accepted Manuscripts are published online shortly after acceptance, before technical editing, formatting and proof reading. Using this free service, authors can make their results available to the community, in citable form, before we publish the edited article. We will replace this *Accepted Manuscript* with the edited and formatted *Advance Article* as soon as it is available.

You can find more information about *Accepted Manuscripts* in the [Information for Authors](#).

Please note that technical editing may introduce minor changes to the text and/or graphics, which may alter content. The journal's standard [Terms & Conditions](#) and the [Ethical guidelines](#) still apply. In no event shall the Royal Society of Chemistry be held responsible for any errors or omissions in this *Accepted Manuscript* or any consequences arising from the use of any information it contains.

Application of laser ablation (imaging) inductively coupled plasma mass spectrometry for mapping and quantifying Fe in transgenic and non-transgenic soybean leaves

Cite this: DOI: 10.1039/x0xx00000x

Received 00th January 2012,
Accepted 00th January 2012

DOI: 10.1039/x0xx00000x

www.rsc.org/

Silvana R. Oliveira,^a and Marco A. Z. Arruda^{a*}

A laser ablation inductively coupled plasma mass spectrometry is used for determining Fe in leaves of transgenic (variety M 7211RR) and non-transgenic (variety MSOY 8200) soybean, grown for 21 days in a growth chamber at controlled temperature (27 ± 0.1 °C) and photoperiod (12 h). The same technique, but in the imaging mode, is also employed for acquiring the spatial distribution of Fe in leaves of both varieties. For attaining both proposals, different parameters such as RF power, carrier and auxiliary gas flow rates, dynamic reaction cell flow rate, RPq, laser intensity, spot diameter, frequency and scan speed are optimized. The accuracy of the laser ablation method is accessed by comparing the results (from ratios between ^{56}Fe and ^{13}C , used as an internal standard) obtained from pellet samples (200 mg of the certified reference materials – NIST SRM 1515 and 1573a at 7 psi of pressure), or prepared pellets from transgenic and non-transgenic soybean leaves, with those from digested samples. No differences at 95% confidence levels are found. Although Fe concentrations are similar comparing transgenic and non-transgenic leaves, its spatial distribution is greatly different. While Fe is homogeneously distributed in the whole transgenic soybean leaf, this element is greatly concentrated in the main vein and nerves of the non-transgenic leaf. Taken into account the all variables are controlled during the experiment, this result indicates that genetic modification may be altering the Fe distribution in the soybean leaves.

Introduction

The high consumption and application of soybean due to its cost and appreciated nutritional and functional properties are motivating improvements in the cultivation and increase of the worldwide production. The growth in the soybean production can be significantly attributed to the widespread cultivation of transgenic plants once the genetic modification is one of the most effective strategies to obtain higher yields.^{1,2} The Roundup Ready® soybean from Monsanto tolerates the herbicide glyphosate, and it is the most well-known and used transgenic soybean product owing to cost efficiencies for weed control and elevated yield.³ In spite of the extensive cultivation of Roundup Ready® soybean plants around the world, their use as human and animal food is controversial due to uncertainties about their safety and equivalence with respect to conventional soybean. Comparative studies involving transgenic (T) and non-transgenic (NT) soybeans have revealed the presence of changes in the proteome, enzymes and metalloproteins of transgenic seeds, and in the proteome and enzymes of transgenic leaves.⁴⁻¹⁰ The genetic modification can be providing not only tolerance to herbicide but also causing changes in the metabolism of T plants. Iron, which among the essential micronutrients in plants

is required at greatest abundance, presents higher concentration in T (variety MSOY 7575 RR) than NT soybean seeds (variety MSOY 7501).⁶ On the other hand, there is little information¹¹ about possible differences in Fe distributions among different compartments of T and NT soybean plants such as leaves, for example.

Typically, the direct element imaging such as laser ablation imaging inductively coupled plasma mass spectrometry [LA(i)-ICP-MS] in plant tissues is more reliable than bulk analysis since it is not affected by sample preparation, which may modify the element distribution. The direct imaging of essential, beneficial, and toxic metals in biological tissues require techniques with good spatial resolution and high signal/noise ratio (low detection limits) due to their natural heterogeneous distributions.¹² Laser ablation inductively coupled plasma mass spectrometry (LA-ICP-MS) is a powerful analytical technique to map the distribution of metals/metalloids and non-metals in environmental and biological samples as well as in plant tissues. Multielemental analysis, high sensitivity and easy sample preparation are among its main advantages^{13,14} whereas the quantitative analysis, probably, is the most challenging step.^{15,16} The calibration and accuracy are often affected due to matrix

1 differences between the samples and certified reference
2 materials.^{15,16}

3 The reliable Fe determination by ICP-MS is usually hindered
4 by spectral interferences, and the Ar- and Ca-based molecular
5 ions are the most problematic ones. The main interferences that
6 hamper the accurate ⁵⁶Fe measurement are ⁴⁰Ar¹⁶O and
7 ⁴⁰Ca¹⁶O.¹⁷ Despite of the absence of water in the LA-ICP-MS
8 system in reducing these polyatomic interferences on ⁵⁶Fe,
9 molecules such as O₂, CO₂ and H₂O impurities are present in
10 the carrier gas.¹⁸ Additionally, Ca is a macronutrient currently
11 present in leaf tissues, from 1.5 to 5.0 % mass fraction range,
12 which can correspond *ca.* 130-185 times the Fe concentration
13 (around 80 and 400 μg g⁻¹).

14 Although the use of the dynamic reaction cell (DRC)
15 technology can eliminate or minimize the Ar- and Ca-based
16 interferences, its use is not common in LA-ICP-MS due to the
17 reduction in the analyte signal intensity. However, the use of H₂
18 as a reaction gas can promote the chemically induced
19 dissociation by means of ion-molecule interactions. When
20 using H₂, the interfering species can experience hydrogen atom
21 transfer, proton transfer or charge transfer.¹⁸ The H₂ is known
22 for reacting rapidly with ArO⁺ and slowly with Fe⁺. Recently,
23 the H₂ was used as a reaction gas to eliminate high polyatomic
24 background signals for LA-ICP-MS imaging of various
25 elements in mouse brain, including Fe.¹⁸ With a H₂ flow rate of
26 3.0 mL min⁻¹, a significant decrease in analyte background
27 levels, and in the limits of analysis, as well as an increase in
28 signal-to-noise ratios and in image quality were observed for
29 Fe.¹⁸

30 Then, this paper describes a method for evaluating the
31 distribution of Fe in T and NT soybean leaves employing
32 LA(i)-ICP-MS as well as for determining this micronutrient in
33 plant materials by LA-ICP-MS. Two different certified
34 reference materials of plants were used to validate the method,
35 and the Hydrogen was used as a reaction gas to promote the
36 chemically induced dissociation of the interferences, improving
37 the analytical performance of the imaging of Fe.

38 Experimental

39 Reagents, materials and equipment

40 All solutions were prepared in polypropylene flasks with
41 deionized water (≥ 18.2 MΩ cm) from a Milli-Q water
42 purification system (Millipore, USA). All reagents used for
43 sample preparation were from Merck (Darmstadt, Germany).
44 Nitric and hydrochloric acids from Merck were purified in a
45 sub-boiling system (Berghof, Germany) before using. Iron
46 standard solution (1000 mg L⁻¹) was purchased from Merck.
47 The working standard solution used to pellet preparation was
48 prepared from the stock solution by simple dilution with Milli-
49 Q water. The CRMs (1515 Apple Leaves and 1573a Tomato
50 Leaves) from the National Institute of Standards and
51 Technology (NIST) were used for optimization and validation
52 of the method. Ultra-clean procedures were used for sample
53 preparation and analysis. Plastic bottles and glassware were
54 cleaned by soaking in 10% (v/v) HNO₃ at least 24 h and rinsed
55 abundantly in de-ionized water before use.

56 A quadrupole-based ICP-MS equipped with a cyclonic spray
57 chamber and a Meinhard nebulizer as well as a dynamic
58 reaction cell (Elan DRC-e, PerkinElmer) and coupled to a laser
59 ablation system (New Wave UP 213) was used in the
60 quantification procedure and for imaging Fe distributions in T
and NT soybean leaves. The LA system was equipped with a

solid state Nd:YAG laser at 213 nm. The ablated material was
transported towards to ICP using argon as the carrier gas. An
optimized hydrogen gas flow was introduced into the dynamic
reaction cell to eliminate the interferences on the ⁵⁶Fe isotope.
The software MatLab version 7.13 was used to build-up the
images of the scanned leaves and correlate the obtained signals
with the concentrations of Fe in the leaves.

61 Transgenic and non-transgenic soybean

62 Transgenic (variety M 7211 RR) and NT (variety MSOY 8200)
63 soybean seeds were kindly donated by Monsanto (Brazil). The
64 T soybean presents resistance to the herbicide glyphosate-N-
65 (phosphonomethyl)glycine. For handling the Roundup Ready®
66 type T soybean seeds, the Institute of Chemistry has a Biosafety
67 Quality Certificate (issued on July 24, 2007; number 240/2007).
68 Transgenic and NT soybean seeds were germinated and grown
69 in plastic pots (200 mL capacity) containing a mixture of 50%
70 (m/m) substrate (BasaPlant, Brazil) plus 50% (m/m)
71 vermiculite (Vermfloc Agro, Brazil) with pH of 6.2. The
72 germination took about 3 days, and the plants were allowed to
73 grow for 21 days in a growth chamber under a controlled
74 temperature (27 ± 0.1 °C) and photoperiod (12 h), and the
75 plants were irrigated daily using deionized water. Forty eight
76 plants were cultivated, being 24 T and 24 NT. The youngest
77 leaves were collected from the upper region of the plants after
78 21 days of cultivation to directly evaluate the distribution of Fe
79 in these structures. The other leaves were used as matrix source
80 for preparing the standards in the validation procedure.

81 Validation of the quantification procedure and analysis of 82 transgenic and non-transgenic leaves by LA-ICP-MS

83 The proposed procedure for Fe quantification used pellets of
84 the certified reference materials (NIST SRM 1515 Apple
85 Leaves and NIST SRM 1573a Tomato Leaves) and pellets of
86 the T and NT soybean leaves. The pellets were prepared
87 pressing 200 mg of the CRM (previously homogenized during
88 10 min in a mortar and pestle and allowed to stand for 48 h) at
89 7 psi, and were fixed onto double-sided adhesive tape in the LA
90 chamber. For building-up the calibration curves, each pellet
91 was spiked with 0, 100, 300, 400 and 500 μg g⁻¹ of Fe, by
92 adding 500 μL of Fe standard solution with different
93 concentrations to 200 mg of CRM. The soybean leaves were
94 pressed under the same conditions as the CRMs.

95 Firstly, a pellet of the certified reference material of tomato
96 leaves and a leaf of soybean were used to optimize the
97 instrumental parameters of the laser ablation and ICP-MS
98 systems. The parameters optimized such as laser intensity (%),
99 spot diameter (μm), frequency (Hz) and scan speed (μm s⁻¹),
100 RF power (W), carrier gas flow rate (argon- L min⁻¹), auxiliary
101 gas flow rate (argon - L min⁻¹) and the dynamic reaction cell
102 gas flow rate (Hydrogen - mL min⁻¹) and RPq (V) were then
103 evaluated. Prior to pellet and leaf ablations, gas blank signals
104 for the m/z 13 and 56 were collected to obtain the background
105 signals.

106 With the instrumental parameters optimized, which are
107 described in Table 1, the Fe concentration was determined in
108 the certified reference material of apple leaves by standard
109 addition calibration method.

Table 1. Optimized instrumental parameters for Fe determination by ICP-MS and LA-ICP-MS. The integration time for each point is determined by multiplying the dwell time by the number of sweeps. The resolution on the Y axis is given by the distance between two successive lines, while on the X axis is determined by multiplying the scan speed by the acquisition time for each point

	LA-ICP-MS	ICP-MS (digested samples)
Rf power (W)	1300	1240
Carrier gas flow rate – Ar (L min ⁻¹)	0.90	0.91
Auxiliary gas flow rate – Ar (L min ⁻¹)	1.80	1.10
Reading mode	Peak Hopping	Peak Hopping
Integration time (ms)	50	50
Sweeps/reading	3	50
Integration time (ms)	150	2500
Detector Dead time (ns)	60	60
Replicates	Variable	5
Acquisition time for each point (s)	0.324	----
Monitored Isotopes	¹³ C and ⁵⁶ Fe	⁵⁶ Fe
Dynamic Reaction cell parameters		
H ₂ gas flow (mL min ⁻¹)	2.0	0.4
Rp _q (V)	0.7	0.7
Laser ablation system		
Wavelength of Nd:YAG laser (nm)		213
Frequency (Hz)		15
Laser Intensity (%)		45
Average energy output (mJ)		0.040
Average fluence (J cm ²)		0.41
Spot diameter (μm)		50
Resolution – X axis (μm)		16.2
Resolution – Y axis (μm)		100

After determining the Fe concentration in the CRM of apple leaves, the pellets were used for standard calibration, allowing the quantification of Fe in the CRM of tomato leaves and in T and NT leaves for validating the proposed analytical procedure. The apple leaves CRM standards were measured first with five lines each in randomly selected regions by LA-ICP-MS (Table 1) and, then, the pellets of the CRM of tomato leaves and of T and NT leaves. The ¹³C and ⁵⁶Fe intensities were measured by LA-ICP-MS. The ¹³C was used as the internal standard to compensate the water content effect and possible variations in the ablation process, which can be related to the heterogeneity of the prepared standards or changes in the ablation process itself.¹⁹ The ratio of the ⁵⁶Fe ion intensity to that of ¹³C was plotted against the concentration of the spike in the prepared standard in order to build-up the calibration curve.

Following the analysis via LA-ICP-MS, the pellets prepared with T and NT leaves as well as those with certified reference

materials (without standard addition) were decomposed using a microwave oven. The pellets were digested with a mixture of 2.0 mL of H₂O₂, 3.5 mL of HNO₃ and 0.50 mL of HCl in closed PTFE vessels submitted to the following microwave program: 5 min at 240 W; 5 min at 420 W; 5 min at 600 W and 15 min at 800 W. After digestion, all samples were filtered and the volumes adjusted to 25 mL with deionized water. The Fe determination by ICP-MS was performed after further dilutions of the samples with the standard sample introduction system, consisting of a cyclonic spray chamber and a Meinhard nebulizer, according to the conditions shown in Table 1.

The prepared standards of the CRM of apple leaves were also used for standard calibration during Fe distribution in T and NT soybean leaves. The standards were scanned first with five lines each in randomly selected regions by LA-ICP-MS and then the T and NT leaves were scanned line by line (Table 1). Regarding resolution, the distance between successive lines in the leaves was set to 100 μm. The leaves were dried at 40 °C until constant weight to reduce the possible signal variations during the analyses owing to changes in water content and also increase in the amount of ablated material introduced into the mass spectrometer.

Results and discussion

Optimization of the measurement parameters for quantitative imaging of Fe by LA-ICP-MS

Aiming to obtain reliable quantitative images of Fe in T and NT soybean leaves, the laser ablation and ICP-MS parameters were optimized analyzing a pellet of the certified reference material of tomato leaves and a leaf of soybean. The concentration of Fe in the tomato leaves CRM is relatively high (368 ± 7 μg g⁻¹) and significant signals were obtained. Five lines were measured in different regions of the pellet (for each condition evaluated) in order to verify the Fe distribution heterogeneity generated in the pellet production. Each line was measured for 25 s, which corresponded to 1250 μm in length, generating an appropriate number of replicates (around 50). The relative standard deviations for the ratio between ⁵⁶Fe and ¹³C intensities varied from 1.6 to 16.9%. These values demonstrated not only a satisfactory level of homogeneity in the Fe distribution, but also confirm the adequate production of pellet for posterior LA analysis. For this optimization, the unvaried mode was used. The Hydrogen was employed (initially at a low flow rate 0.4 mL min⁻¹) as reaction gas in the dynamic reaction cell (DRC).

The ratio ⁵⁶Fe/¹³C did not varied significantly with the variation of the laser ablation and ICP-MS parameters. This finding underline the suitability of carbon for signal normalization showing that ¹³C was suitable as internal standard since compensates for instrumental and ablation process variations. The laser intensity of 45% was the most adequate while avoiding cutting off the leaf. The laser spot diameter of 55 μm offered the best resolution taking into account the analysis time that was ≥ 10 h for one soybean leaf. The 15 Hz of laser frequency was suitable with the scan speed used (50 μm s⁻¹), which allowed the best ablation performance taking into account the analysis. The sensitivity for the ⁵⁶Fe/¹³C ratio was slight improved with the increase of the RF power used until 1300 W and therefore, this RF was chosen for further experiments. The carrier and auxiliary gases flow rates were also optimized in order to obtain an efficient transport of the ablated material and a stable plasma. The 0.9 mL min⁻¹ of carrier and 1.8 mL min⁻¹ of auxiliary gas flow rates were the

best conditions, once that allowed the most efficient transport of the ablated material. On the other hand, lower flow rates generated unstable plasma.

The dynamic reaction cell gas flow rate (Hydrogen - mL min⁻¹) and RPq (V) were also optimized in order to overcome the spectral interferences under the ⁵⁶Fe (⁴⁰Ar¹⁶O and ⁴⁰Ca¹⁶O). Firstly, the H₂ flow rates were evaluated (0.0; 0.4; 0.8; 1.2; 1.6 and 2.0 mL min⁻¹) with the RPq fixed at 0.7 V, and then the RPq values (0.4; 0.5; 0.6; 0.7; 0.8 and 0.9 V) were tested, maintaining the H₂ flow rate at 2 mL min⁻¹. The background signals for ⁵⁶Fe and ¹³C obtained from the gas blank at different H₂ flow rates are presented in the Figure 1. For ⁵⁶Fe, a noteworthy reduction in the background signal can be observed as the H₂ flow rate increased from 0.0 to 2.0 mL min⁻¹ achieving almost zero for 2.0 mL min⁻¹ (Figure 1a). The increase in H₂ flow rates enhanced the cell pressure and caused a higher number of ion-molecule interactions, probably resulting in the dissociation and removal of the Ar-based polyatomic interferences.^{18,20}

For ¹³C, a significant increase in the background signal can be observed in the Figure 1b as the H₂ flow rate increased from 0.0 to 0.4 mL min⁻¹, indicating the formation of the interfering specie ¹²CH⁺ in the reaction cell ($C^+ + H_2 \rightarrow CH^+ + H$). The relatively high abundance of ¹²C⁺ generated from CO₂ impurities in the plasma gas contributed for the formation of ¹²CH⁺, as it was observed by Lear *et al.* when using hydrogen as a reactive gas in an octapole collision/reaction cell.¹⁸ As the H₂ flow rate gradually increased (from 0.4 to 2.0 mL min⁻¹), the cell pressure also increased causing a higher number of collisions. As a result, a reduction in the kinetic energy of the ion beam probably occurred and allowed the increase in the fragmentation reaction of ¹²CH⁺, which greatly reduced the background signals.

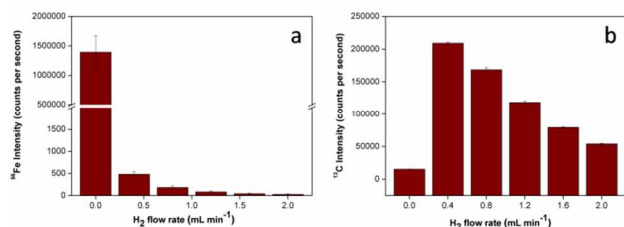


Figure 1. Background signal intensities for (a) ⁵⁶Fe and (b) ¹³C at different H₂ flow rate (mL min⁻¹) conditions.

The ⁵⁶Fe/¹³C ratio, which is obtained from the net signals of ⁵⁶Fe and ¹³C (after blank subtraction), for the certified reference material of tomato leaves did not change significantly with the increase of the H₂ flow rate until 1.6 mL min⁻¹ (see Figure 2). At 0.0 mL min⁻¹ (reaction cell off), the ⁵⁶Fe/¹³C ratio was slightly higher than for the other flow rates, except for 2.0 mL min⁻¹. Although the sensitivity seems better in this case, there is the hypothesis that the ⁴⁰Ca¹⁶O interference is enhancing the ⁵⁶Fe signal. Other possibility is that the signal drift affected the ⁵⁶Fe/¹³C ratio, generating inaccurate results. The signal drift observed for ⁵⁶Fe was higher when the reaction cell was off because it is mainly affected by the background signal (⁴⁰Ar¹⁶O), which was high and fluctuating due to the variations in the concentration of oxygen in the ICP during the analytical process. At 2.0 mL min⁻¹, the ⁵⁶Fe/¹³C ratio was higher than for the other flow rates because the ⁵⁶Fe signal was slight higher whereas ¹³C signal suffered reduction in this flow rate, probably

due to the larger number of collisions in the reaction cell. The signal to noise ratio for ⁵⁶Fe/¹³C improved significantly as the H₂ flow rate increased (Figure 2) since the interferences were reduced. Thus, the 2.0 mL min⁻¹ was chosen for next experiments. Additionally, the limits of detection for the intensity signals of ⁵⁶Fe (LOD = $y_0 + 3s_0$; where y_0 is the average of the gas blank signal, s_0 is the standard deviation of the gas blank signal)²¹ were calculated and it gradually decreased from ca. 2200000 to 68 cps when the H₂ flow rate increased from 0.0 to 2.0 mL min⁻¹. This confirmed the remarkable improvement of the conditions of analysis when the H₂ was used. Then, different H₂ flow rate were necessary when employed LA-ICP-MS (2.0 mL min⁻¹) or ICP-MS (0.4 mL min⁻¹) once that C was measured in the LA system, while in the ICP-MS system this element (C) was not our target.

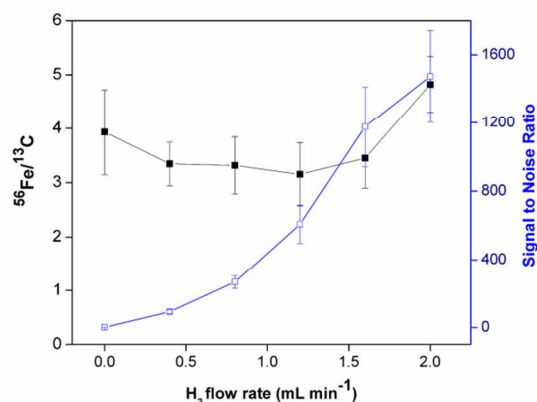


Figure 2. ⁵⁶Fe/¹³C ratio and the signal to noise ratio for ⁵⁶Fe/¹³C versus H₂ flow rate (mL min⁻¹) for the certified reference material of tomato leaves.

Aiming to maximize the transmission of the analyte ions and minimize the passage of interferences to the mass analyzer and detector, the appropriate mass bandpass of the quadrupole field was optimized by means of the RPq parameter (the Mathieu parameter q is proportional to the ELAN parameter RPq). The background signals for ⁵⁶Fe from the gas blank suffered a slight reduction as the RPq voltage increased from 0.4 to 0.9 V, achieving almost zero for 0.9 V. This result indicates that the interference ⁴⁰Ar¹⁶O become more unstable when the voltage applied to the quadrupole reaction cell increased. On the other hand, an increase in the background signal of ¹³C was observed as the RPq voltage increased from 0.4 to 0.8 V, and reduced at 0.9 V. In a different way from the Ar-based interference, ⁴⁰Ar¹⁶O, the ¹³C and the ¹²C⁺H ions (formed in the reaction cell due to the presence of hydrogen) become more stable with the increase of the RPq. Despite of the increase in the background signal of ¹³C, precise results were obtained, since the concentration of hydrogen probably remained invariable during the analytical process, allowing the use of ¹³C as internal standard.

The ⁵⁶Fe and ¹³C signals decreased in the 0.4 – 0.7 V range and as the reduction was not proportional the ⁵⁶Fe/¹³C ratio reduced. At 0.8 and 0.9 V, the ⁵⁶Fe signal continued to decrease, but the ¹³C signal decreased deeply, allowing ⁵⁶Fe/¹³C ratio enhancement. The stability of the ions ⁵⁶Fe was reduced in the 0.4 – 0.7 V range of RPq similarly as occurred for the polyatomic interference ⁴⁰Ar¹⁶O. Despite of this stability reduction, the signal to noise ratio for ⁵⁶Fe/¹³C improved

significantly as the RPq voltage increased from 0.4 to 0.7 V (Figure 3), and, therefore, the 0.7 V was chosen for the next experiments.

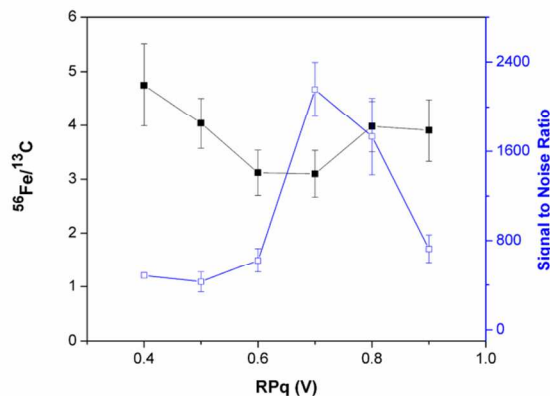


Figure 3. $^{56}\text{Fe}/^{13}\text{C}$ ratio and the signal to noise ratio for $^{56}\text{Fe}/^{13}\text{C}$ versus RPq (V) for the certified reference material of tomato leaves

Accuracy check of the analytical procedure and quantitative imaging of Fe in soybeans leaves by LA-ICP-MS

The concentration of Fe in the certified reference material NIST SRM 1515 Apple Leaves was determined by standard addition method employing LA-ICP-MS. Another certified reference material NIST SRM 1547 Tomato Leaves was used to validate the analytical procedure. In the standard addition method, $^{56}\text{Fe}/^{13}\text{C}$ ratios were obtained in different regions of the NIST SRM 1515 Apple Leaves pellets as a function of Fe concentration. Calibration curve was built-up with the prepared pellets of NIST SRM 1515 Apple Leaves for Fe determination in the NIST SRM 1573a Tomato Leaves. Linear correlation coefficient (> 0.9972) was obtained for 100 - 500 $\mu\text{g g}^{-1}$ Fe concentration range, indicating that the proposed procedure for pellet preparation as well as the strategy adopted for data collection and treatment was adequate.

As presented in the Table 2, the found concentration was in agreement with the certified value at 95% confidence level according the paired *t*-test. The found results for two certified reference materials of leaves were also in agreement with those obtained after microwave digestion and Fe determination by ICP-MS (Table 2). These results confirm the accuracy of the developed method to quantify Fe directly in solid samples. This agreement also confirms the efficient reduction of $^{40}\text{Ar}^{16}\text{O}$ and $^{40}\text{Ca}^{16}\text{O}$ interferences to levels that did not hinder the Fe determination even with the high concentrations of Ca in these CRMs. The precision of the measurements using the hyphenation LA-ICP-MS was poorer than that one obtained using microwave digestion and analysis of solutions by ICP-MS as it was expected according the data published in the literature for plant matrices,^{16,22} once the homogeneity to aqueous solutions is at molecular level.

It is important to emphasize that the concentration of Fe present in the certified reference material NIST SRM 1515 Apple Leaves ($81 \pm 9 \mu\text{g g}^{-1}$) was taken into account as the lowest limit for the calibration curve, and, therefore, the quantification is possible only from this concentration. This was a limiting factor for Fe determination at low concentrations since it is present in all plant matrices.

Table 2. Results obtained for the accuracy check of the method for determination of Fe by LA-ICP-MS. Values represent the average and the standard deviation for measurements ($n = 5$).

Sample	Certified Value ($\mu\text{g g}^{-1}$)	Microwave digestion ICP-MS ($\mu\text{g g}^{-1}$)	LA-ICP-MS ($\mu\text{g g}^{-1}$)
SRM 1515 (Standard Addition)	83 ± 5	80 ± 2	81 ± 9
SRM 1573a (Pellets)	368 ± 7	371 ± 4	390 ± 29
T leaves (Pellets)	----	133 ± 2	138 ± 7
NT leaves (Pellets)	----	134 ± 1	138 ± 8

The Fe concentration in the prepared pellets of soybean leaves were also determined and agreed with the values obtained after microwave digestion and analysis by ICP-MS as also demonstrated in the Table 2. The Fe concentration in soybeans tissues may vary considerably depending on its bioavailability in the soil as well as the characteristics of the soil where the plant is cultivated. In this case, for these two soybean varieties, T (variety M 7211 RR) and NT (variety MSOY 8200), which were cultivated under the same conditions (described before), the found concentrations of Fe in the leaves were not significantly different.

Two-dimensional quantitative images of Fe in T and NT soybean leaves (harvested after 21 days of cultivation) were done and can be seen in the Figure 4. Each leaf itself is also shown in the left side and the images produced by LA-ICP-MS correlates well with the pictures of the leaves. The advantage of using H_2 in the reaction cell was also demonstrated by the improved quality of the images obtained as already reported in the literature for Fe.¹⁸ The use of H_2 dramatically reduced the background signal, not only improving the resolution of the images, but also avoiding errors in the calculated analyte concentration which was less influenced by the signal drift.

Even though the T and NT soybean leaves have equivalent concentrations of Fe, as statistically attested, the Fe distribution profiles in these leaves were greatly different. For the T soybean, the distribution of Fe was basically homogeneous in the whole leaf, being slightly concentrated at the central part and in the tip, achieving high levels (*ca.* 200 $\mu\text{g g}^{-1}$). On the other hand, Fe was mainly concentrated at the main vein and nerves of the NT leaf, achieving *ca.* 100-150 $\mu\text{g g}^{-1}$ in the nerves and 200 $\mu\text{g g}^{-1}$ in the main vein. Lower Fe contents were observed in the regions without veins.

The Fe concentrations in both leaves were comparable with those ones obtained with the pellets. Regarding Fe spatial distribution differences found in T and NT soybeans, previous investigations dealing with this task were not found in the literature and, thus, it is not possible to compare the found results. Comparing with other plant species, an enrichment of Fe in the veins of tobacco leaves, such the observed for NT soybean leaf, was also found by Becker *et al.*²³ Additionally, taking into account the fact that *ca.* 80% of the Fe in plants is found in the chloroplasts¹⁴, it is possible to suppose that some alterations in these organelles may be occurring in the T leaf. Iron is a component of Fe-S clusters, which compose the active sites of many enzymes in plant tissues that are involved with photosynthesis in the chloroplasts.²⁴

Considering that the cultivation conditions were carefully controlled, the same soil was used for both soybean varieties, and that the NT plant had a similar behavior with another plant

species, it is likely the genetic modification may be the cause of the found differences, as already previously demonstrated by different works published by our research group.⁴⁻¹⁰

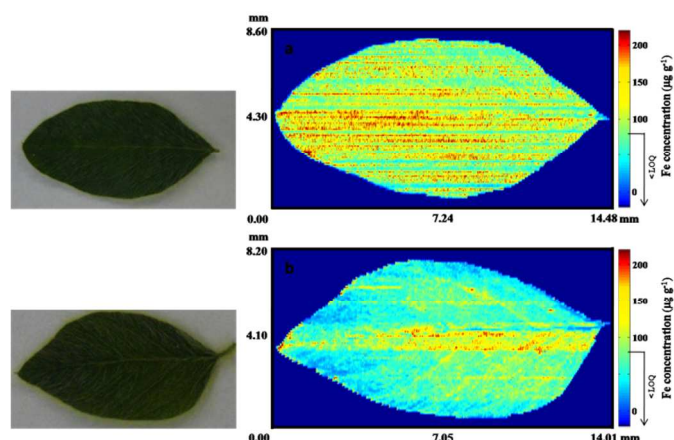


Figure 4. Fe distributions in the (a) T and (b) NT soybean leaves, cultivated under the same condition during 21 days. The picture of each leaf analyzed is shown on the left side of the image.

Conclusions

The initial purpose of mapping and quantifying Fe in T and NT soybean leaves was greatly attained. Although the mass/charge ratio of ⁵⁶Fe presents large number of polyatomic interferences, excellent accuracy of the method was obtained with the strategies adopted in this work. Then, for avoiding these interferences, not only a correctly optimization of the ICP-MS and LA was carried out, but also ¹³C was used as internal standard for compensating signal fluctuations during the ablation process. Additionally, H₂ was an excellent alternative in the dynamic reaction cell of the ICP-MS instead ammonia, which is currently indicated in the literature, once that H₂ was also prone of eliminating polyatomic interferences in the Fe determination by ICP-MS. Finally, this work demonstrates that LA(i)-ICP-MS and LA-ICP-MS are noteworthy techniques for micro and spatial analyses (in the qualitative or quantitative modes), once that they provided the differentiation between T and NT leaves, showing a different Fe spatial distribution, even though its concentration being similar in both soybean varieties.

Acknowledgements

The authors thank the Fundação de Amparo a Pesquisa do Estado de São Paulo (FAPESP grant no. 2011/12054-2 São Paulo, Brazil), the Conselho Nacional de Desenvolvimento Científico e Tecnológico (CNPq, Brasília, Brazil), and the Coordenação de Aperfeiçoamento de Pessoal de Nível Superior (CAPES, Brasília, Brazil) for the financial support and fellowship.

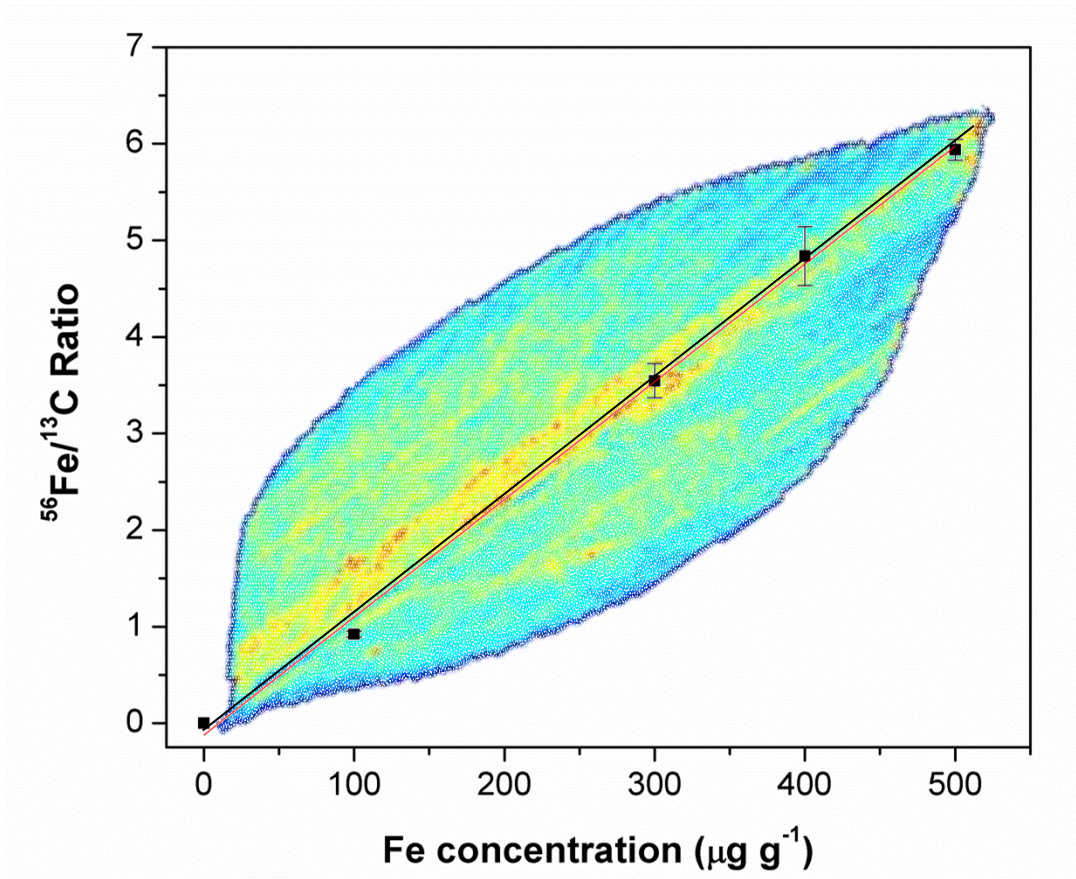
Notes and references

^a Spectrometry, Sample Preparation and Mechanization Group – GEPAM and National Institute of Science and Technology for Bioanalytics - INCTBio, Institute of Chemistry, Department of Analytical Chemistry, University of Campinas - Unicamp, PO Box 6154, Zipcode 13083-970, Campinas, SP, Brazil.

* Corresponding Author

E-mail: zezzi@iqm.unicamp.br

- P. Westcott, USDA Agricultural Projections to 2019, Inter-agency Agricultural Projections Committee, U.S. Department of Agriculture, 2010. U.S. Department of Agriculture. <http://www.ers.usda.gov/publications/oce-usda-agricultural-projections/oce-2010-1.aspx#Ukm3uoZJOSo>, (accessed Feb 2014).
- Monsanto do Brasil, <http://www.monsanto.com.br>, (accessed Feb 2014).
- S. Natarajan, D. Luthria, H. Bae, D. Lakshman and A. Mitra, *J. Agric. Food Chem.*, 2013, **61**, 11736–11743.
- A. Sussulini, G. H. M. F. Souza, M. N. Eberlin and M. A. Z. Arruda, *J. Anal. At. Spectrom.*, 2007, **22**, 1501–1506.
- A. R. Brandão, H. S. Barbosa and M. A. Z. Arruda, *J. Proteomics*, 2010, **73**, 1433–1440.
- L. R. V. Mataveli, P. Pohl, S. Mounicou, M. A. Z. Arruda and J. Szpunnar, *Metallomics*, 2010, **2**, 800–805
- L. R. V. Mataveli, M. Fioramonte, F. C. Gozzo and M. A. Z. Arruda, *Metallomics*, 2012, **4**, 373–378.
- H. S. Barbosa, S. C. C. Arruda, R. A. Azevedo and M. A. Z. Arruda, *Anal. Bioanal. Chem.*, 2012, **402**, 299–314.
- M. A. Z. Arruda, R. A. Azevedo, H. S. Barbosa, L. R. V. Mataveli, S. R. Oliveira, S. C. C. Arruda and P. L. Gratão, in *A Comprehensive Survey of International Soybean Research – Genetics, Physiology, Agronomy and Nitrogen Relationships*, ed. J. E. Board, InTech, New York, 2013, ch. 27, pp. 583–613.
- S. C. C. Arruda, H. S. Barbosa, R. A. Azevedo and M. A. Z. Arruda, *J. Proteomics*, 2013, **93**, 107–116.
- S. R. Oliveira, A. A. Menegário, M. A. Z. Arruda, *Metallomics*, DOI: 10.1039/c4mt00162a.
- J. S. Becker, M. Zoriy, A. Matush, B. Wu, D. Salber, C. Palm, J. S. Becker, *Mass. Spectrom. Rev.*, 2010, **29**, 156–175.
- J. Cizdziel, B. Kaixuan, P. Nowinski, *Anal. Methods*, 2012, **4**, 564–569.
- B. Wu, F. Andersch, W. Weschke, H. Weberb, J. S. Becker, *Metallomics*, 2013, **5**, 1276–1284.
- J. S. Becker, *Inorganic Mass Spectrometry. Principles and Applications*, Wiley, First Edition, 2007.
- M. A. O. Silva, M. A. Z. Arruda, *Metallomics*, 2013, **5**, 62–67.
- F. Vanhaecke, L. Balcaen, G. Wannemacker, L. Moens, *J. Anal. At. Spectrom.*, 2002, **17**, 933–943.
- J. Lear, J. D. Hare, F. Fryer, P. A. Adlard, D. I. Finkelstein, P. A. Doble, *Anal. Chem.*, 2012, **84**, 6707–6714.
- B. Wu, Y. Chena, J. S. Becker, *Anal. Chim. Acta*, 2009, **633**, 165–172.
- P. B. Armentrout, *J. Anal. At. Spectrom.*, 2004, **19**, 571–580.
- D. C. Harris, *Quantitative Chemical Analysis*, W. H. Freeman and Co., New York City, 6th ed.; 2002.
- B. Wu, M. Zoriy, Y. Chen, J. S. Becker, *Talanta*, 2009, **78**, 132–137.
- J. S. Becker, R. C. Dietrich, A. Matusch, D. Pozebon, V. L. Dressler, *Spectrochim. Acta B*, 2008, **63**, 1248–1252.
- A. Kötschau, G. Büchel, J. W. Einax, C. Fischer, W. von Tümpling, D. Merten, *Microchem. J.*, 2013, **110**, 783–789.



1
2
3
4
5
6
7
8
9
10
11
12
13
14
15
16
17
18
19
20
21
22
23
24
25
26
27
28
29
30
31
32
33
34
35
36
37
38
39
40
41
42
43